Title:
Quickly-responding C-fiber nociceptors contribute to heat hypersensitivity in the area of secondary hyperalgesia

Authors and affiliations:
Cédric Lenoir [1], Léon Plaghki [1], André Mouraux [1] and Emanuel N. van den Broeke [1]*

1: Institute of Neuroscience, Université catholique de Louvain, Brussels, Belgium.

*Corresponding author:
Emanuel N van den Broeke
Institute of Neuroscience (IoNS)
Université catholique de Louvain
B-1200, Brussels
Belgium
E-mail: Emanuel.vandenbroeke@uclouvain.be

Additional information:

Competing interest
None declared.

Author contribution
CL, LP, AM and ENvdB have contributed to the conception and design of the experiment. CL and ENvdB contributed to the data acquisition and analysis. CL, ENvdB, LP and AM contributed to the interpretation of the data and approved the final version of the manuscript.

Funding
CL and AM are supported by the ERC "Starting Grant" (PROBING PAIN 336130). ENvdB is supported by the ERC "Starting Grant" (PROBING PAIN 336130) and the Fonds de Recherche Clinique (FRC).

Short biography

Cédric Lenoir is currently in the latest stage of his PhD in the laboratory of André Mouraux at the Institute of Neuroscience of the Université catholique de Louvain headed by Prof. André Mouraux. His work focuses, in humans, on the central and peripheral mechanisms involved in nociception in normal condition and during sensitization in particular in the area of secondary hyperalgesia. His

work aiming at better characterizing these mechanisms could have potential contribution to chronic pain conditions.

Key points:

- A recent animal study showed that high frequency electrical stimulation (HFS) of C-fibers induces a gliogenic heterosynaptic LTP at the spinal cord which is hypothesized to mediate secondary hyperalgesia in humans.
- Here we tested this hypothesis by predominantly activating C-fibers nociceptors in the area of secondary mechanical hyperalgesia induced by HFS in humans.
- We show that heat perception elicited by stimuli predominantly activating C-fiber nociceptors is greater, as compared to the control site, after HFS in the area of secondary mechanical hyperalgesia.
- This is the first study that confirms in humans the involvement of C-fiber nociceptors to the changes in heat sensitivity in the area of secondary mechanical hyperalgesia induced by HFS.

Abstract

It has recently been shown that high frequency electrical stimulation (HFS) of C-fibers induces a gliogenic heterosynaptic long term potentiation (LTP) at the spinal cord in animals, which has been hypothesized to be the underlying mechanism of secondary hyperalgesia in humans. Here we tested this hypothesis using a method to predominantly activate quickly-responding C-fiber nociceptors in the area of secondary hyperalgesia induced by HFS in humans. HFS was delivered to one of the two volar forearms in 18 healthy volunteers. Before, 20 minutes and 45 minutes after HFS short lasting (10 ms) high intensity CO_2 laser heat stimuli delivered to a very small area of the skin (0.15 mm^2) were applied to the area of increased mechanical pinprick sensitivity at the HFS treated arm and the homologous area of the contralateral control arm. During heat stimulation the electroencephalogram, reaction times (RT) and intensity of perception (NRS 0-100) were measured. After HFS, we observed a greater heat sensitivity, an enhancement in the number of detected trials, faster RT and an enhancement of the N2 wave of C-fiber LEPs at the HFS treated arm compared to the control arm. This is the first study that confirms in humans the involvement of C-fiber nociceptors to enhanced heat sensitivity in the area of secondary mechanical hyperalgesia induced by HFS.

INTRODUCTION

Previous in vitro studies have shown that high-frequency electrical stimulation (HFS) of primary C-fiber afferents induces synaptic long-term potentiation (LTP) between these peripheral C-fibers and spinal lamina I neurons projecting to the parabrachial area in the brainstem (Ikeda et al., 2003). More recently, it has been shown that HFS of primary C-fiber afferents also triggers glial cell activation which, via the release of diffusible extracellular messenger, including D-serine and tumor necrosis factor (TNF), can induce

LTP at remote C-fiber synapses (Kronschläger et al., 2016). Based on these results it is hypothesized that activity-dependent homosynaptic LTP within spinal nociceptive pathways contributes to primary hyperalgesia, whereas glia-mediated heterosynaptic LTP would explain secondary hyperalgesia, i.e. the increased pain sensitivity beyond the area of injury.

In humans, HFS delivered onto the skin to activate peripheral nociceptors induces a pronounced increase in mechanical pinprick sensitivity in the surrounding unconditioned skin (Klein et al., 2004; Henrich et al., 2015; Van den Broeke et al., 2016). Studies have suggested that this heterotopic increase of mechanical pinprick sensitivity is abolished during A-fiber nerve conduction blockade (Ziegler et al., 1999), and is still present in skin pre-treated with capsaicin to induce denervation of capsaicin-sensitive afferents (Magerl et al., 2001). Based on these results, it was hypothesized that secondary mechanical hyperalgesia is mediated by either A-fiber high-threshold mechanoreceptors (A-HTM) or slowly-adapting A-fiber mechano- and heat-sensitive nociceptors (AMH Type I), as these two categories of A-fiber nociceptors are mechano-sensitive and insensitive to capsaicin (Ringkamp et al., 2001). In a more recent study, we showed that the responses to long-duration heat stimuli known to activate AMH Type I were not enhanced after HFS, indicating that the secondary mechanical hyperalgesia observed in humans after HFS is predominantly mediated by A-HTMs (van den Broeke et al., 2016).

Nonetheless, after HFS, brief CO_2 laser stimuli heating the skin above the threshold of heat-sensitive A- and C-fiber nociceptors are perceived as more intense when delivered to the surrounding unconditioned skin (van den Broeke and Mouraux, 2014a). Such short-lasting heat stimuli can be expected to preferentially activate quickly-responding

AMH Type II (Treede et al., 1998) and quickly-responding C-fiber mechano-heat nociceptors (CMH; Meyer and Campbell, 1981; Wooten et al., 2014). Therefore, the increased sensitivity to short-lasting heat stimuli following HFS could be the result of an enhancement of the responses elicited by the activation of these nociceptors.

We have recently showed that the perception elicited by intra-epidermal electrical stimulation (IES) does not change when IES is applied inside the area of secondary hyperalgesia induced by HFS (Buirrun Manresa et al., 2018). IES delivered at low intensities selectively activates Aδ-fiber nociceptors and the responses are believed to be mainly related to AMH type II nociceptors (Mouraux et al., 2010; Liang et al., 2016). The lack of effect of HFS on the perception elicited by stimuli selectively activating Aδ-fiber nociceptors leaves open the intriguing question whether the changes in heat perception after HFS are mediated by C-fiber nociceptors, which would be compatible with the results obtained in animals by Kronschläger et al. (2016).

A previous study has investigated the effect of HFS on heat-sensitive C-fibers in humans. In that study low-intensity heat stimuli (43°C on average) were used to selectively activate heat-sensitive C-fibers having a lower heat activation threshold than AMH (van den Broeke and Mouraux, 2014b). Such low-intensity heat stimuli can be expected to predominantly activate warm-sensitive C-fibers rather than CMH. Indeed, LaMotte and Campbell (1978) showed, using single fiber recordings in primates, that heating the skin to 43°C induces a strong discharge in C-fiber warm receptors and almost no response in CMH.

Here, we use a different approach to specifically test, in humans, the after-effects of HFS on the responses elicited by the activation of quickly-responding C-fibers. Bragard et al.

(1996) showed that short-lasting high-intensity CO_2 laser stimuli delivered to a very small area of the skin (0.15 mm^2) predominantly activate C-fibers. Specifically, they showed that such stimuli were detected with very late reaction times and elicited ERPs within a very late time window, compatible with the conduction velocity of unmyelinated C-fibers (Bromm et al. 1983; Bromm and Treede, 1987). The selectivity for C-fibers of such stimuli is explained by the fact that high-intensity stimuli delivered to a tiny area of the skin can be expected to predominantly activate CMH, as these have a much higher skin innervation density than AMH (Plaghki and Mouraux 2002). Furthermore, it can be expected that such stimuli will only rarely also activate C-warm receptors. Indeed, C-warm receptors have very small punctate receptive fields (Hensel and Iggo, 1971; Lamotte and Campbell, 1978; Duclaux and Kenshalo, 1980; Hallin et al., 1982) and are very sparsely distributed in human skin (Hallin et al., 1982; Torebjörk et al., 1996). Further supporting this, Green and Cruz (1998) showed that in humans the forearm has large areas that are warm-insensitive (≥5 cm^2). Therefore, high stimulation temperatures delivered to a *tiny* area of the skin can be expected to predominantly activate quickly-responding C-fiber nociceptors, with little or no concomitant activation of AMH and C-warm afferents.

In the present study, we use this method to specifically assess the possible contribution of quickly-responding C-fiber nociceptors to the HFS-induced changes in heat sensitivity in the area of secondary hyperalgesia in humans.

METHODS AND MATERIALS

Ethical Approval

The experiment was conducted according to the lastest version of the Declaration of Helsinki, except for registration in a database. Approval for the experimental procedures was obtained by the Ethics Committee (Commission d'Éthique Biomédicale Hospitalo-Facultaire) of the Université catholique de Louvain (UCL) (B403201316436). All participants were informed of the experimental procedures and provided a written informed consent form and were financially compensated for their participation.

Participants

Eighteen healthy volunteers (13 women/5 men; 23.3 ± 3.4 years; mean ± SD; range 19 - 34) took part in the experiment.

Procedure

The design of the experiment is summarized in Figure 1. All participants were blinded to the aim of the study and naïve with the procedures. During the experiment, participants were comfortably seated in an adjustable chair with the tested arm resting on a pillow on a table in front of them. The view of the arm was prevented during the experiment.

High frequency electrical stimulation of the skin

Transcutaneous high frequency electrical stimulation of the skin (HFS) was used to induce secondary hyperalgesia. Several studies have shown that this method induces a

robust and long-lasting increase in mechanical pinprick sensitivity, extending beyond the area of stimulation (Klein et al., 2004; Pfau et al., 2011; Henrich et al., 2015; van den Broeke et al., 2016). HFS was applied on the left or right volar forearm, 10 cm distal to the cubital fossa, and consisted of five trains of 100 Hz (pulse width: 2 ms), each lasting 1 s. The time interval between each train was 10 s. The intensity of stimulation was individually adjusted to 20 times the detection threshold to a single pulse (0.3 ± 0.06 mA, mean ± SD). The electrical pulses were triggered by a programmable pulse sequencer (Master-8; AMPI Israel), generated by a constant current electrical stimulator (Digitimer DS7A, Digitimer UK), and delivered to the skin using a specifically designed electrode built at the Centre for Sensory-Motor Interaction (Aalborg University, Denmark). The electrode consists of 16 blunt stainless steel pins (diameter: 0.2 mm) protruding 1 mm from the base. The pins are placed in a 10 mm diameter circle and serve as cathode. A stainless steel anode electrode is concentrically located around the steel pins (inner diameter: 22 mm; outer diameter: 40 mm; Fig. 1B). To avoid any confounding effect of handedness, the arm onto which HFS was applied (dominant vs. non dominant) was counterbalanced across participants. Handedness was assessed using the Flinders Handedness Survey (Nicholls et al., 2013).

Predominant activation of quickly-responding C-fiber nociceptors

Heat stimuli were generated by an infrared CO_2 laser (wavelength 10.6 µm; Department of Physics, Université catholique de Louvain, Belgium) controlled by adjusting the laser power output (20 steps extending between 0 – 0.22 W). A lens (zinc-selenide, diameter: 25.4 mm, focal length: 127 mm, Edmund Optics, Barrington, New Jersey) specially designed for this wavelength was used to focus the 10 mm diameter laser beam to a diameter at target site of approximately 0.3 mm (Fig. 2). The intensity of stimulation

(HFS arm: 10.4 ± 3.2 mJ/mm^2; control arm: 10.3 ± 3.2 mJ/mm^2, mean ± SD) was adjusted individually for each arm by increasing the power output by 2 steps above the value obtained for the heat detection threshold, corresponding to an approximate increase of 4 mJ/mm^2. The heat detection threshold was determined at the beginning of the experiment using a staircase procedure based on the detection of the stimulus (Churyukanov et al., 2012). Participants were requested to press a button held in the contralateral hand as soon as they detected the heat stimulus.

In order to characterize the temporo-spatial profile of the heat stimulus, we measured the skin temperature with an infrared camera (1 kHz sampling rate, FLIR SC7500, FLIR, Nashua, US) at the target site of the heat stimulation in one participant (Fig 2B.D.E.). The intensity of stimulation was set to the average intensity of stimulation used across participants (1.04 mJ). As shown in Figure 2B, a peak temperature of 79.5°C was reached. Because of the Gaussian profile of the laser beam and the spatial resolution of the images obtained by the infrared camera (one pixel = 0.1×0.1 mm), the actual maximum skin temperature at the center of the beam was probably higher than the temperature measured by the image pixel exhibiting maximum temperature. Indeed, the value of 79.5°C represents the average temperature within that pixel. Nevertheless, the maximum temperature probably never exceeded 100°C as no vaporization was observed during any of the trials. Most importantly, the peak temperature was clearly above the thermal activation threshold of both CMH (Namer et al., 2009; Meyer and Campbell, 1981; Treede et al., 1995; Weidner et al. 1999; Wooten et al. 2014) and AMH-II nociceptors (Treede et al., 1995; 1998). The beam diameter estimated using the full width at half-maximum temperature was 0.34 mm. The beam diameter was also estimated based on the area of the skin where temperature exceeded 43°C, which is

slightly above the average heat activation threshold of CMH (Namer et al., 2009; Meyer and Campbell, 1981; Treede et al., 1995; Weidner et al., 1999; Wooten et al., 2014; Fig. 2D). The diameter of the area of the skin that exceeded 43°C was 0.30 mm. In order to estimate the actual temperature increase at the epidermal layers of the skin we used a finite element analysis of heat transfer to the skin (Marchandise et al., 2014). As shown in Figure 2B, the simulation predicted correctly the skin surface temperature measured by the infrared camera. Assuming that the thickness of the epidermal layer of the hairy skin of the forearm is, on average, 50 μm, the model estimated a peak temperature of 59.2°C at the dermoepidermal junction (Fig. 2C).

Quantifying changes in mechanical pinprick sensitivity

To confirm the successful induction of secondary hyperalgesia, mechanical pinprick stimuli (128 mN; MRC Systems, Heidelberg, Germany) were applied inside the test area of both forearms, before and 45 minutes after HFS (measurement T2). At each measurement, three pinprick stimuli were delivered onto the skin and participants were asked to report the perceived intensity elicited by the three pinprick stimuli on a numerical rating scale (NRS) ranging from 0 (no perception) to 100 (maximal pain), with 50 representing the transition from non-painful to painful domains of sensation. To avoid sensitization of the stimulated skin, the target of each pinprick stimulus was displaced after each stimulus. The arm onto which the pinprick stimuli were applied first was counterbalanced across participants.

Quantifying changes in heat sensitivity

To assess after-effects of HFS on heat sensitivity, the same stimuli as described above but at an intensity just above the threshold were delivered before HFS (T0), 20 minutes

after HFS (T1) and 45 minutes after HFS (T2) in the test area of both forearms. At each measurement a minimum of thirty stimuli were given in order to obtain at least 20 valid trials (i.e. trials with a reaction time ≥ 650 ms; Churyukanov et al., 2012; Mouraux et al., 2003; van den Broeke and Mouraux, 2014b). RTs to each stimulus were collected at each measurement during the experiment. Trials were sorted in three categories relatively to their corresponding RT: (1) trials at which the stimulus was undetected or with a RT > 2500 ms, (2) trials at which the stimulus was detected with a RT < 650 ms and (3) trials at which the stimulus was detected with a RT ≥ 650 ms. The inter-stimulus interval ranged from 7 to 10 s. After each stimulus, participants were asked to verbally rate the perceived intensity using the NRS described above. During the entire experiment, participants listened to white noise delivered through earphones and the view of the arm was prevented. To avoid nociceptor habituation and/or sensitization, the position of the arm was changed by the experimenter such as to displace the target site of the laser stimuli by approximately 2 cm after each stimulus. After each displacement, the distance between the lens and the arm was readjusted to correspond to the focal length.

EEG recording

During the heat sensitivity assessment, the EEG was recorded using a 32 channels system with an average reference (1 kHz sampling rate; 32-channel ASA-LAB EEG system; Advanced Neuro Technologies, The Netherlands), with 32 actively shielded Ag-AgCl electrodes mounted in an elastic electrode cap and arranged according to the International 10-20 system (Waveguard32 cap; Advanced Neuro Technologies). Participants were instructed to keep their gaze fixed and to sit as still as possible. Eye

movements were recorded using two adhesive surface electrodes placed at the upper-left and lower-right sides of the left eye. Impedances were kept below 5 kΩ for all leads.

EEG analysis

The EEG was processed offline using Letswave 6 (http://www.nocions.org/letswave6). The EEG signal was bandpass-filtered using a 0.5 to 30 Hz zero-phase Butterworth filter (Bragard, 1995; Opsommer et al., 2003; van den Broeke and Mouraux, 2014b). The signal was then segmented in 3 s epochs extending from -500 to +2500 ms relative to the onset of the heat stimuli. Only the epochs in which the stimulus was detected with a RT compatible with the conduction velocity of C fiber nociceptors were processed. Artefacts related to eye movements and eye blinks were removed using a method based on an Independent Component Analysis (FastICA algorithm; Hyvarinen and Oja 2000). After baseline correction (reference interval -500 to 0 ms), the signal was re-referenced to the average of the left and right earlobe channels. Epochs with signals exceeding ±75 μV were considered as artefact and rejected. Remaining epochs (23 ± 3) were averaged for each participant, stimulation site and time point. C-fiber laser-evoked potentials (CLEPs) were defined as in previous studies (Bragard et al., 1996; Jankovski et al., 2013). Two distinct peaks were identified (N2 and P2; Figure 3). Because of the large inter-individual variability of the latencies of the N2 component thought to be mainly due to differences in peripheral conduction distances, a large time window ranging from +350 to +1200 ms relative to stimulation onset was used to identify the maximum negative (N2) and positive (P2) peaks within each averaged waveform.

Statistical analysis

Statistical analyses were performed using SPSS 24 (SPSS, Chicago, IL, USA).

To assess the effect of HFS on mechanical pinprick perception, a two-way repeated measures analysis of variance (RM-ANOVA) was performed. *Time* (T0 and T2) and *arm* (control vs. HFS arm) were used as within-subject factors. The average value of the three pinprick stimuli was used as dependent variable.

To assess the effect of HFS on the intensity of perception elicited by the small-surface heat stimuli, reaction times ≥ 650 ms, the proportion of trials with a RT ≥ 650 ms and N2 and P2 amplitudes and latencies, each dependent variable was analysed using a two-way repeated measures analysis of variance (RM-ANOVA) with *time* (T0, T1 and T2) and *arm* (control vs. HFS arm) as within-subject factors. In addition, we also analysed the proportion of trials detected with a RT < 650 ms and the proportion of undetected trials.

The assumption of sphericity was tested using Mauchly's test. In case the data violated the assumption of sphericity, F-values were corrected using the Greenhouse-Geisser procedure (denoted $F_{G\text{-}G}$). The effects of HFS were further assessed using planned contrasts ("simple" method). When needed post-hoc tests consisting of paired t-tests corrected for multiple comparisons were performed. The level of significance was set at $p < 0.05$ (two-sided).

RESULTS

Perception

Mechanical pinprick sensitivity

HFS induced a clear increase in mechanical pinprick sensitivity on the HFS arm (Fig. 5A, B). The RM-ANOVA revealed a significant interaction between the factors *time* and *arm* ($F_{(1,17)}$=99.78; p<.001; η^2=.854). Post hoc comparisons (paired t-tests) showed a significant increase in pinprick perception after HFS at the HFS treated arm ($t_{(17)}$=9.255; p<.001), while pinprick perception was not significantly different after HFS at the control arm.

C-fiber nociceptor-evoked heat sensitivity

The RM-ANOVA revealed a significant *time* × *arm* interaction ($F_{(2,34)}$=10.81; p<.001; η^2=.389) for the perception elicited by the transient heat stimuli. The univariate within-subject contrasts showed a significant interaction between the factors *time* and *arm*, both 20 minutes after HFS (T1: $F_{(1,17)}$=14.25; p=.002; η^2=.456) and 45 minutes after HFS (T2: $F_{(1,17)}$=13.26; p=.002; η^2=.438, Fig. 5C, D). Post-hoc paired t-tests revealed that the intensity of perception observed at the control arm was significantly decreased relative to T0, both at T1 ($t_{(17)}$=4.565; p=.0015) and at T2 ($t_{(17)}$=5.181; p<.001). No significant change in perceived intensity was observed at the HFS-treated arm.

Reaction times

The distribution of the reaction times across all participants and conditions is shown in Fig. 6A.

Reaction times compatible with the detection of C-fiber input (RT ≥ 650 ms). When specifically assessing RTs compatible with C-fiber conduction velocities, the RM-ANOVA revealed a marginally significant *time × arm* interaction ($F_{G\text{-}G\ (1.41,24.01)}$=3.975; p=.050; η^2=.183). This interaction was clearer when considering the multivariate test statistics, which do not rely on the assumption of sphericity ($F_{(2,16)}$=9.841; p=.002; η^2=.552). The univariate within-subject contrasts showed a significant interaction at T1 ($F_{(1,17)}$=20.904; p<.001; η^2=.551), but not at T2 (Fig. 6B, C). Post hoc paired t-tests showed that RTs were significantly reduced at T1 compared to T0 at the HFS arm ($t_{(17)}$=4.764; p<.001), but not at the control arm.

The mean proportion of undetected trials or trials with a RT larger or shorter than 650 ms for all conditions are shown in Fig. 7A.

The RM-ANOVA also revealed a significant *time × arm* interaction for the proportion of trials detected with a reaction time compatible with C-fiber conduction velocities ($F_{G\text{-}G\ (1.32,22.37)}$=8.126; p=.006; η^2=.323). The univariate within-subject contrasts showed a significant interaction at T1 ($F_{(1,17)}$=11.851; p=.003; η^2=.411) and T2 ($F_{(1,17)}$=8.271; p=.010; η^2=.327; Fig. 7B). Post hoc paired t-tests showed that the proportion of trials with a RT ≥ 650 ms significantly decreased at T2 ($t_{(17)}$=4.163; p=.0028) but not T1 (p=.277) as compared to T0 at the control arm while there was no significant change at T1 ($t_{(17)}$=2.529; p=.085) and T2 (p=.976) at the HFS arm.

Reaction times compatible with the detection of A-fiber input (RT < 650 ms). When specifically assessing the proportion of trials detected with a RT compatible with A-fiber conduction velocities, the RM-ANOVA did not reveal a significant *time × arm* interaction ($F_{(2,34)}$=.759; p=.476; η^2=.043; Fig 7C).

Undetected trials. The RM-ANOVA revealed a significant *time × arm* interaction on the proportion of undetected trials ($F_{G\text{-}G\ (1.46,24.71)}$=11.134; p=.001; η^2=.396). The univariate within-subjects contrasts further showed a significant interaction at T1 ($F_{(1,17)}$=10.412; p=.005; η^2=.380) and T2 ($F_{(1,17)}$=13.781; p=.002; η^2=.448; Fig 7D). Post hoc paired t-tests showed a significant increase in the proportion of undetected trials at T2 ($t_{(17)}$=4.096; p<.001) compared to T0, but not at T1 compared to T0, for the control arm. No significant change in the proportion of undetected trials was observed at the HFS arm.

Laser-evoked brain potentials related to the predominant activation of C-fiber nociceptors

Because we noticed a large inter-subject variability in the latency of LEPs (Fig. 3B), individual waveforms were aligned to the individual latency of the N2 wave for visualization purposes only. The aligned group-level average waveforms of trials detected with a reaction time ≥ 650 ms are shown in Figure 3A. Non-aligned group-level average LEPs waveforms are shown in Figure 4).

The RM-ANOVA performed on the magnitude of the N2 peak revealed a significant *time × arm* interaction ($F_{(2,34)}$=6.171; p=.005; η^2=.266). The univariate within-subjects contrasts further showed a significant interaction at T1 ($F_{(1,17)}$=9.010; p=.008; η^2=.346) and T2 ($F_{(1,17)}$=8.647; p=.009; η^2=.337, Fig 8A, B). Post hoc paired t-tests revealed a significant increase of the magnitude of the N2 wave at T1 ($t_{(17)}$=4.864; p<.001) but not at T2 (p=.125) as compared to T0 at the HFS arm. No significant change in N2 wave magnitude was observed at the control arm.

The RM-ANOVAs performed on the magnitude of the P2 peak ($F_{(2,34)}$=1.633; p=.210; η^2=.088, Fig 8C, D), the latency of the N2 peak ($F_{(2,34)}$=.817; p=.450; η^2=.046, Table 1)

and the latency of the P2 peak ($F_{(2,34)}$=1.445; p=.250; η^2=.078, Table 1) revealed no significant interaction.

DISCUSSION

Here we provide novel data, obtained in humans, supporting the hypothesis that increased heat sensitivity in the area of secondary hyperalgesia is mediated, at least in part, by quickly-responding C-fiber nociceptors. Indeed, when high intensity small-surface area CO_2 laser stimuli predominantly activating C-fiber nociceptors are delivered to the area of secondary hyperalgesia induced by HFS, we observe a greater heat sensitivity (as compared to control site), an increase in the number of detected trials, and faster reaction times. Furthermore, we observe an enhancement of the N2 wave of C-fiber LEPs.

Type of C-fibers activated by high intensity tiny surface CO_2 laser stimuli

Here we show similarly to Bragard et al. (1996) that CO_2 laser heat stimuli delivered to tiny cutaneous surface areas can selectively activate heat-sensitive C-fibers. Indeed, the reaction times and the latency of the LEPs are compatible with the conduction velocity of unmyelinated fibers (Otsuru et al., 2009). Important to note, the difference in LEP N2 latency between the study of Bragard et al. (1996) and the present study can be explained by the different conduction distances related to the different body parts that were stimulated (hand dorsum vs. volar forearm). The LEPs of the present study are not related to the activation of Aδ-fiber nociceptors. Indeed, as can be seen in the Figure 4,

stimuli detected with a RT compatible with Aδ-fiber nociceptors conduction velocities elicited an earlier latency LEP (average N2 latency across conditions 171 ms).

Studies have suggested that functionally different classes of C-fiber nociceptors exist (Meyer and Campbell, 1981; Schmidt et al., 1995; Weidner et al. 1999; Wooten et al., 2014). For example, both Meyer and Campbell (1981) and Wooten et al. (2014) identified using standard teased-fiber recordings in monkeys heat-sensitive C-fiber afferents that responded either quickly or slowly to sustained heat stimuli delivered for several seconds. Quickly-responding C-fiber nociceptors respond relatively quick (within 100 ms) after the onset of the heat stimulus but their rate of discharge fades out very quickly over time. In contrast, the discharge rate of slowly-responding C-fiber nociceptors remains constant throughout the sustained heat stimulus. C-fiber nociceptors have further been distinguished based on the modality of the stimuli to which they respond (mechanical and/or heat). The short-lasting heat stimuli in the present study probably mostly activate quickly-responding heat sensitive C-fiber nociceptors (CMH). However, it is unclear whether such stimuli could also activate mechano-insensitive C-fiber nociceptors (Schmidt et al., 1995; Weidner et al, 1999).

After-effects of HFS on heat perception

Similar to the effect of HFS on the responses to mechanical pinprick stimuli, the effect of HFS on the heat percept elicited by the transient activation of C-fiber nociceptors was long-lasting and involved both T1 and T2. Indeed, while heat perception habituated on the control arm this was not the case for the HFS arm resulting in a greater heat sensitivity as compared to control arm. This greater heat sensitivity was further supported by the significant increase in the number of detected trials at the HFS

treated-arm, at T1 and T2. We also observed faster reaction times after HFS at the HFS treated arm, however, this effect was only present at T1 but not anymore T2. In sum, C-fiber nociceptors contribute to HFS-induced changes in heat sensitivity in the area of secondary hyperalgesia.

After-effects of HFS on ultra-late LEP responses

HFS also had a long-lasting effect on the magnitude of the N2 wave of the LEP elicited by the predominant activation of C-fiber nociceptors. Importantly, other studies have shown that HFS can also enhance the vertex N wave elicited by innocuous short lasting vibrotactile stimuli selectively activating low-threshold mechano-receptors in the area of secondary hyperalgesia (van den Broeke and Mouraux, 2014a), as well as to stimuli selectively activating Aδ-fiber nociceptors (Biurrun Manresa et al., 2018). The enhancement of the N wave elicited by vibrotactile stimuli indicates that HFS can induce effects that are not restricted to the transmission of nociceptive inputs at the level of the spinal cord. Moreover, in the study of Biurrun Manresa et al. (2018) as well as van den Broeke and Mouraux (2014a) the enhancement of the N wave was not accompanied by an increase in intensity of perception suggesting that perception and brain responses are not necessarily related and/or reflect different processes. It has been hypothesized that these brain responses reflect a system that is involved in detecting, orienting attention towards and reacting to the occurrence of salient sensory events (Legrain et al., 2011).

Peripheral versus central sensitization

Using intradermal capsaicin injection, a previous study showed that secondary mechanical hyperalgesia disappears during an A-fiber nerve conduction block (Ziegler

et al., 1999), suggesting that secondary mechanical hyperalgesia is mainly mediated by A- rather than C-fibers. If these results are also applicable to HFS, our results suggest that besides the involvement of A-fiber nociceptors mediating changes in mechanical pinprick sensitivity, there is also a sensitized C-fiber pathway mediating changes in heat sensitivity.

There is currently no convincing evidence for a peripheral sensitization of CMH in the area of secondary hyperalgesia (Baumann et al., 1991; Schmelz et al., 1996; Schmelz et al., 2000; Serra et al., 2004). However, Serra et al. (2004), using microneurography, found that mechano-insensitive C-fiber nociceptors can become responsive to both mechanical and heat stimulation after remote intradermal capsaicin injection. It is currently not known whether HFS induces a peripheral sensitization of this population of fibers in the area of secondary hyperalgesia through a spreading of neurogenic inflammation, nor whether these afferents can be activated by short-lasting heat stimuli once they have been sensitized.

Interestingly, Kronschläger et al. (2016) recently showed in animals that HFS of primary C-fiber afferents triggers glial cells activation, and that this glial activation can induce LTP at remote C-fiber synapses via the release of diffusible extracellular messengers, including D-serine and TNF. According to the authors, this mechanism may account for the secondary hyperalgesia following tissue injury or inflammation in humans. The present study shows that C-fiber nociceptors contribute to changes in heat sensitivity in the area of secondary hyperalgesia in humans, which could well be explained by the mechanism identified by Kronschläger et al. (2016) in animals.

REFERENCES

Baumann TK, Simone DA, Shain CN & LaMotte RH. (1991). Neurogenic hyperalgesia: the search for the primary cutaneous afferent fibers that contribute to capsaicin-induced pain and hyperalgesia. J Neurophysiol 66, 212-227.

Biurrun Manresa J, Kaesler Andersen O, Mouraux A, & van den Broeke E. (2018). High frequency electrical stimulation induces a long-lasting enhancement of event-related potentials but does not change the perception elicited by intra-epidermal electrical stimuli delivered to the area of secondary hyperalgesia. bioRxiv 282335; DOI: 10.1101/282335.

Bragard D (1995). Perception and neurophysiological correlates of brief infrared laser pulses: influence of cutaneous stimulation area. Doctoral thesis. Université catholique de Louvain, Faculté de médecine, Institut d'éducation physique et de réadaptation, Brussels, Belgium.

Bragard D, Chen AC, Plaghki L. (1996). Direct isolation of ultra-late (C-fibre) evoked brain potentials by CO2 laser stimulation of tiny cutaneous surface areas in man. Neurosci Lett 209 (2), 81-84.

Bromm B, Neitzel H, Tecklenburg A, Treede RD. (1983). Evoked cerebral potential correlates of C-fibre activity in man. Neurosci Lett 43 (1), 109-114.

Bromm B, Treede RD. (1987). Pain related cerebral potentials: late and ultralate components. Int J Neurosci 33 (1-2), 15-23.

Churyukanov M, Plaghki L, Legrain V & Mouraux A. (2012). Thermal detection thresholds of Adelta- and C-fibre afferents activated by brief CO2 laser pulses applied onto the human hairy skin. PLoS One 7, e35817.

Darian-Smith I, Johnson KO, LaMotte C, Kenins P, Shigenaga Y, Ming VC. (1979). Coding of incremental changes in skin temperature by single warm fibers in the monkey. J Neurophysiol 42 (5), 1316-1331.

Duclaux R & Kenshalo DR, Sr. (1980). Response characteristics of cutaneous warm receptors in the monkey. J Neurophysiol 43, 1-15.

Green BG & Cruz A. (1998). "Warmth-insensitive fields": evidence of sparse and irregular innervation of human skin by the warmth sense. Somatosens Mot Res 15, 269-275.

Hallin RG, Torebjork HE & Wiesenfeld Z. (1982). Nociceptors and warm receptors innervated by C fibres in human skin. J Neurol Neurosurg Psychiatry 45, 313-319.

Henrich F, Magerl W, Klein T, Greffrath W & Treede RD. (2015). Capsaicin-sensitive C- and A-fibre nociceptors control long-term potentiation-like pain amplification in humans. Brain 138, 2505-2520.

Hensel H & Iggo A. (1971). Analysis of cutaneous warm and cold fibres in primates. Pflugers Arch 329, 1-8.

Hyvärinen A, Oja E. (2000). Independent component analysis: algorithms and applications. Neural Netw 13 (4-5), 411-430.

Ikeda H, Heinke B, Ruscheweyh R, Sandkühler J. (2003). Synaptic plasticity in spinal lamina I projection neurons that mediate hyperalgesia. Science 299, 1237-1240.

Jankovski A, Plaghki L and Mouraux A. (2013). Reliable EEG response to the selective activation of C-fiber afferents using a temperature-controlled infrared laser stimulator in conjunction with an adaptive staircase algorithm. Pain 154 (9), 1578-1587.

Klein T, Magerl W, Hopf HC, Sandkuhler J & Treede RD. (2004). Perceptual correlates of nociceptive long-term potentiation and long-term depression in humans. J Neurosci 24, 964-971.

Kronschläger MT, Drdla-Schutting R, Gassner M, Honsek SD, Teuchmann HL, Sandkühler J. (2016). Gliogenic LTP spreads widely in nociceptive pathways. Science 354 (6316), 1144-1148.

LaMotte RH, Campbell JN. (1978). Comparison of responses of warm and nociceptive C-fiber afferents in monkey with human judgments of thermal pain. J Neurophysiol 41 (2), 509-258.

Legrain V, Iannetti GD, Plaghki L, Mouraux A. (2011). The pain matrix reloaded: A salience detection system for the body. Prog Neurobiol 93 (1), 111-124.

Liang M, Lee MC, O'Neill J, Dickenson AH, Iannetti GD. (2016). Brain potentials evoked by intraepidermal electrical stimuli reflect the central sensitization of nociceptive pathways. J Neurophysiol 116(2), 286-295.

Magerl W, Fuchs PN, Meyer RA & Treede RD. (2001). Roles of capsaicin-insensitive nociceptors in cutaneous pain and secondary hyperalgesia. Brain 124, 1754-1764.

Marchandise E, Mouraux A, Plaghki L & Henrotte F. (2014). Finite element analysis of thermal laser skin stimulation for a finer characterization of the nociceptive system. J Neurosci Methods 223, 1-10.

Meyer RA, Campbell JN. (1981). Evidence for two distinct classes of unmyelinated nociceptive afferents in monkey. Brain Res 224 (1), 149-152.

Mouraux A, Iannetti GD & Plaghki L. (2010). Low intensity intra-epidermal electrical stimulation can activate Adelta-nociceptors selectively. Pain 150, 199-207.

Namer B, Barta B, Ørstavik K, Schmidt R, Carr R, Schmelz M, Handwerker HO. (2009). Microneurographic assessment of C-fibre function in aged healthy subjects. J Physiol 587 (2), 419-428.

Nicholls ME, Thomas NA, Loetscher T & Grimshaw GM. (2013). The Flinders Handedness survey (FLANDERS): a brief measure of skilled hand preference. Cortex 49, 2914-2926.

Opsommer E, Guérit JM, Plaghki L. (2003). Exogenous and endogenous components of ultralate (C-fibre) evoked potentials following CO2 laser stimuli to tiny skin surface areas in healthy subjects. Neurophysiol Clin 33 (2), 78-85.

Otsuru N, Inui K, Yamashiro K, Miyazaki T, Ohsawa I, Takeshima Y & Kakigi R. (2009). Selective Stimulation of C Fibers by an Intra-Epidermal Needle Electrode in Humans. Open Pain Journal, 53-56.

Pfau DB, Klein T, Putzer D, Pogatzki-Zahn EM, Treede R-D, Magerl W. (2011). Analysis of hyperalgesia time courses in humans after painful electrical high-frequency stimulation identifies a possible transition from early to late LTP-like pain plasticity. Pain 152 (7), 1532-1539.

Plaghki L and Mouraux A. (2002). Brain responses to signals ascending through C-fibers. Int Congress Series 1232, 181-192.

Ringkamp M, Peng YB, Wu G, Hartke TV, Campbell JN & Meyer RA. (2001). Capsaicin responses in heat-sensitive and heat-insensitive A-fiber nociceptors. J Neurosci 21, 4460-4468.

Schmelz M, Schmidt R, Ringkamp M, Forster C, Handwerker HO, Torebjörk HE. (1996). Limitation of sensitization to injured parts of receptive fields in human skin C-nociceptors. Exp Brain Res 109 (1), 141-147.

Schmelz M, Schmid R, Handwerker HO & Torebjork HE. (2000). Encoding of burning pain from capsaicin-treated human skin in two categories of unmyelinated nerve fibres. Brain 123 (3), 560-571.

Schmidt R, Schmelz M, Forster C, Ringkamp M, Torebjörk E, Handwerker H. (1995). Novel classes of responsive and unresponsive C nociceptors in human skin. J Neurosci 15(1), 333-341.

Serra J, Campero M, Bostock H, Ochoa J. (2004). Two Types of C nociceptors in human skin and their behavior in areas of capsaicin-induced secondary hyperalgesia. J Neurophysiol 91, 2770-2781.

Torebjork HE, Schmelz M, Handwerker HO. (1996). Functional properties of human cutaneous nociceptors and their role in pain and hyperalgesia. In: Belmonte C, Cervero F, editors. Neurobiology of nociceptors. p. 349-369. Oxford University Press, Oxford.

Treede RD, Meyer RA & Campbell JN. (1998). Myelinated mechanically insensitive afferents from monkey hairy skin: heat-response properties. J Neurophysiol 80, 1082-1093.

Treede RD, Meyer RA, Raja SN & Campbell JN. (1995). Evidence for two different heat transduction mechanisms in nociceptive primary afferents innervating monkey skin. J Physiol 483 (3), 747-758.

van den Broeke EN, Mouraux A. (2014a). High frequency electrical stimulation of the human skin induces heterotopical mechanical hyperalgesia, heat hyperalgesia and enhanced responses to non-nociceptive vibrotactile input. J Neurophysiol 111, 1564–1573.

van den Broeke EN and Mouraux A. (2014b). Enhanced brain responses to C-fiber input in the area of secondary hyperalgesia induced by high frequency electrical stimulation of the skin. J Neurophysiol 112, 2059–2066.

van den Broeke EN, Lenoir C, Mouraux A. (2016). Secondary hyperalgesia is mediated by heat-insensitive A-fibre nociceptors. J Physiol 594, 6767-6776.

Weidner C, Schmelz M, Schmidt R, Hansson B, Handwerker HO, Torebjörk HE. (1999). Functional attributes discriminating mechano-insensitive and mechano-responsive C nociceptors in human skin. J Neurosci 19 (22), 10184-10190.

Wooten M, Weng HJ, Hartke TV, Borzan J, Klein AH, Turnquist B, Dong X, Meyer RA, Ringkamp M. (2014). Three functionally distinct classes of C-fibre nociceptors in primates. Nat Commun 5, 4122.

Ziegler EA, Magerl W, Meyer RA & Treede RD. (1999). Secondary hyperalgesia to punctate mechanical stimuli. Central sensitization to A-fibre nociceptor input. Brain 122 (12), 2245-2257.

Table 1

	control arm					
	T0		**T1**		**T2**	
	latency (ms)	magnitude (μV)	latency (ms)	magnitude (μV)	latency (ms)	magnitude (μV)
N2	554±99	-7.66±2.55	546±108	-7.39±3.17	562±113	-6.99±2.52
P2	898±95	8.47±2.89	915±97	8.34±2.95	917±97	7.92±2.79

	HFS arm					
	T0		**T1**		**T2**	
	latency (ms)	magnitude (μV)	latency (ms)	magnitude (μV)	latency (ms)	magnitude (μV)
N2	533±86	-6.20±2.14	561±101	-8.40±2.61	531±101	-7.71±3.29
P2	909±82	8.89±2.94	882±62	10.22±4.32	880±55	9.08±3.11

Magnitudes and latencies of the N2 and P2 peaks of LEPs (mean±SD) for each arm at T0, T1 and T2.

Figures captions

Figure 1. Experimental design. **A.** HFS was applied at one of the two volar forearms, 10 cm distally to the cubital fossa. Heat sensitivity and EEG responses to transient stimuli predominantly activating C-fiber nociceptors was assessed at both arms before applying HFS (T0), 20 minutes after applying HFS (T1) and 45 minutes after applying HFS (T2). Mechanical pinprick sensitivity was assessed before applying HFS (T0) and at the end of the experiment after the second measurement (after T2), also at both arms. This sensory testing was performed by delivering the mechanical and heat stimuli to a circular test area (grey ring), located immediately outside the skin area receiving HFS. **B.** HFS of the skin was delivered using a concentric electrode composed of 16 blunt

stainless-steel pins protruding 1 mm from the base and placed in a 10 mm diameter circle and serve as cathode. A stainless-steel anode electrode is concentrically located around the steel pins (inner diameter: 22 mm; outer diameter: 40 mm).

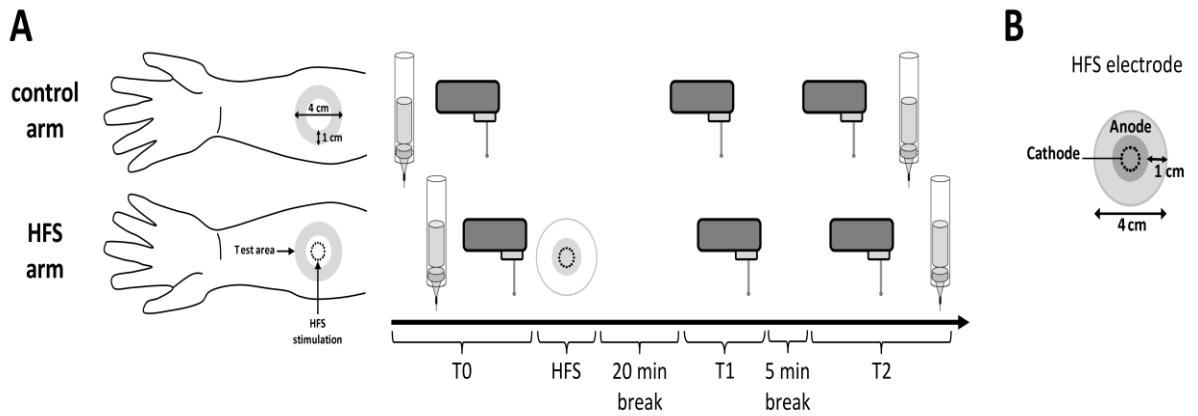

Figure 2. Predominant activation of quickly-responding C-fiber heat sensitive nociceptors was achieved by applying high intensity CO_2 laser pulses focused over a tiny area of the skin. **A.** Using a gold-plated mirror, the laser beam was reflected into a convex focusing lens designed for the emission wavelength of the laser (10.6 μm) to have a focal length of 127 mm. The distance between the lens and the surface of the skin was adjusted such as to correspond precisely to the focal length. This was measured using two visible laser diodes whose target on the skin coincided when the distance corresponded to the focal length. **B.** Time course of the surface temperature of the skin

at target site measured using a high-speed infrared camera (in black). Time course of the surface skin temperature predicted by finite elements modelling of heat transfer to the skin. Note the close correspondence of the prediction of the model with the actual measured surface temperature (maximum 79.5°C). The grey bar represents the transient (10 ms) heat stimulus. Also note that passive cooling of the skin required approximately 800 ms to return to the baseline temperature. **C.** Modelling by finite element analysis of the temperature profile at 50 μm below the skin surface where the free nerve endings terminate in the epidermal layers. Maximum temperature reached at this depth was 59.2°C. **D.** Infared image (spatial resolution: 0.1 × 0.1 mm pixels) of skin temperature at target site when the temperature reached its maximum (image obtained using a high-speed infrared camera in one participant). The actual area at which the temperature exceeded 43°C comprises of seven pixels (outlined by the black line) and covers a total area of .07 mm^2. **E.** Time course of the size of the area in which the temperature exceeded the activation threshold of C-fiber nociceptors (43°C). The time during which the skin remained above this temperature was shorter than 50 ms.

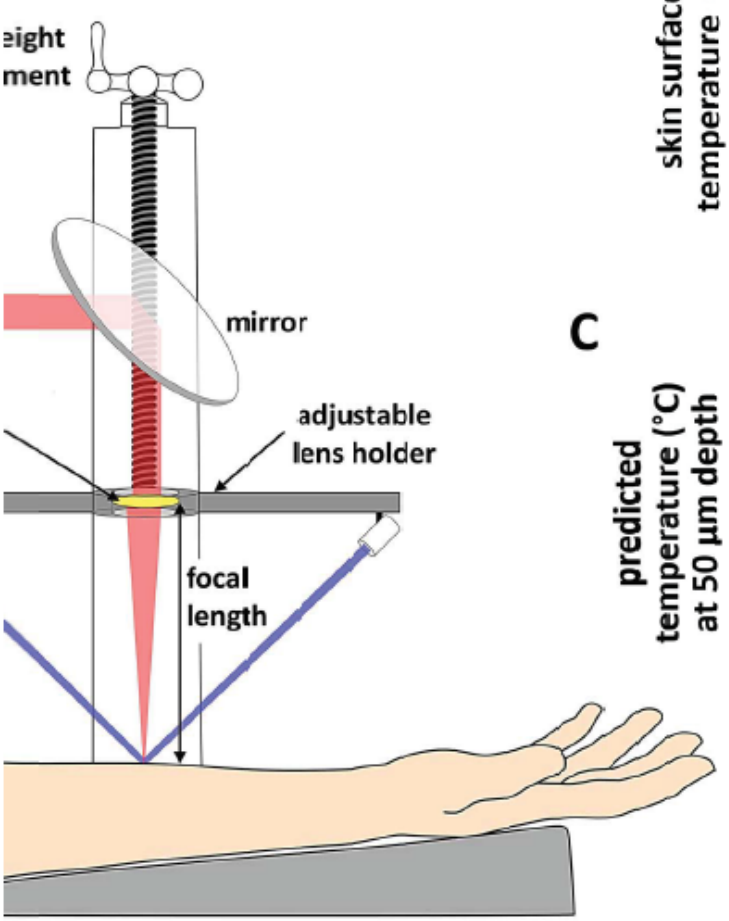

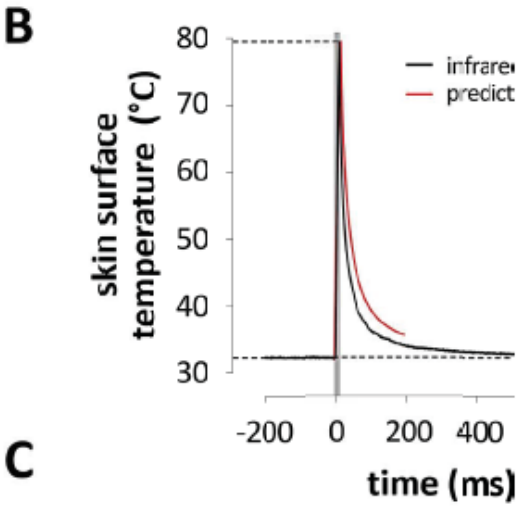

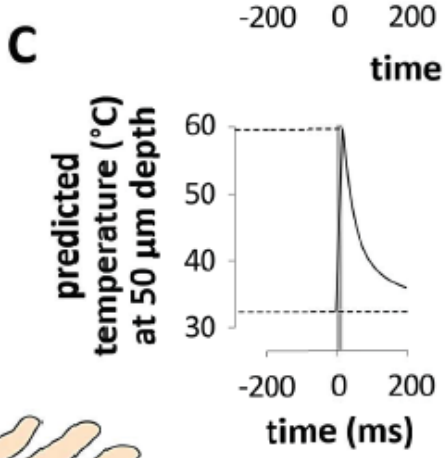

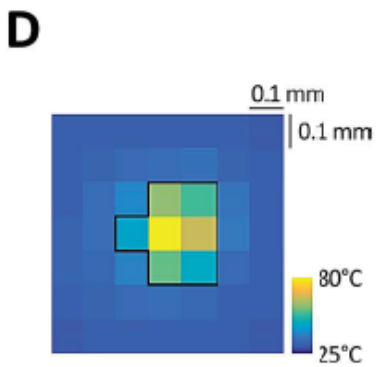

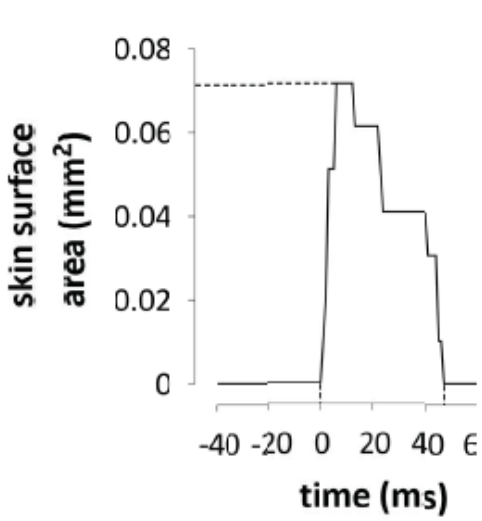

Figure 3. A. Grand-average waveforms of LEPs elicited by the predominant activation of C-fiber nociceptors (electrode Pz vs. A1A2) at the HFS arm and the contralateral control arm, before HFS (T0 in black), 20 minutes after HFS (T1 in red) and 45 minutes after HFS (T2 in blue). To take into consideration interindividual variations in peripheral conduction times, the grand-average waveforms have been computed on the basis of the subject-level average waveform re-aligned relative to the latency of the N2 wave. Note the clear increase of the magnitude of the N2 wave elicited by stimulation of the HFS arm at both T1 and T2. Group-level average scalp topographies are displayed next to the corresponding N2 and P2 waves for both arms and each time point. **B.** Frequency distribution of the latency of the N2 wave across participants and conditions. Note the large inter-individual variability. The mean latency of the N2 wave was 548 ± 100ms.

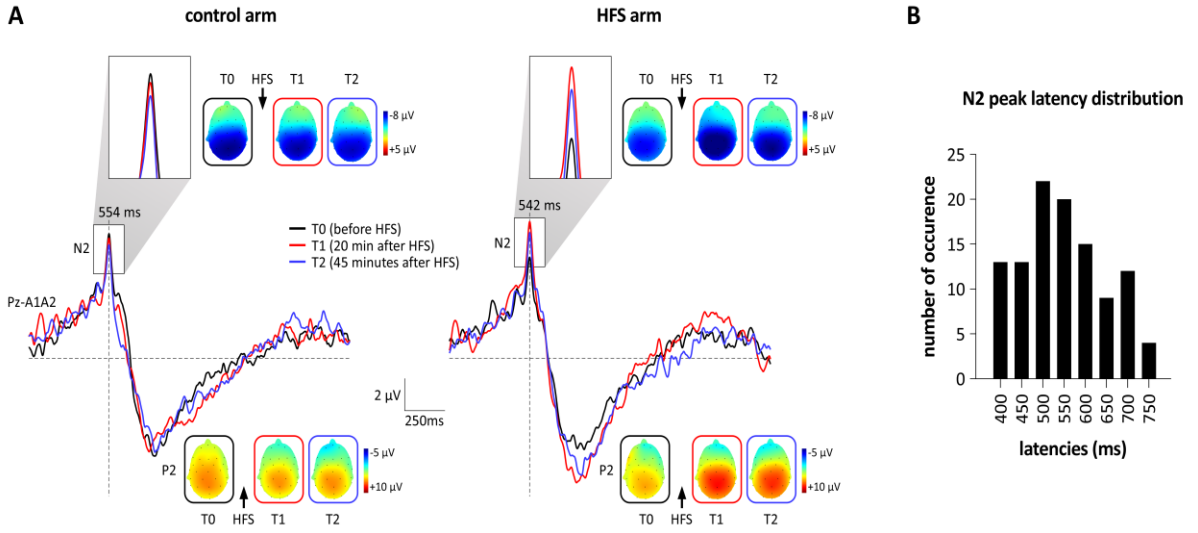

Figure 4. Non-aligned grand-average LEP waveforms elicited by the predominant activation of C-fiber nociceptors (electrode Pz vs. A1A2) at the HFS arm and the contralateral control arm, before HFS (T0 in black), 20 minutes after HFS (T1 in red) and 45 minutes after HFS (T2 in blue). For each arm and across measurements, the non-

aligned grand-average LEP waveforms elicited by stimuli detected with a RT < 650 ms is displayed in grey. Note the earlier latency of the LEPs related to the activation of A-fiber nociceptors.

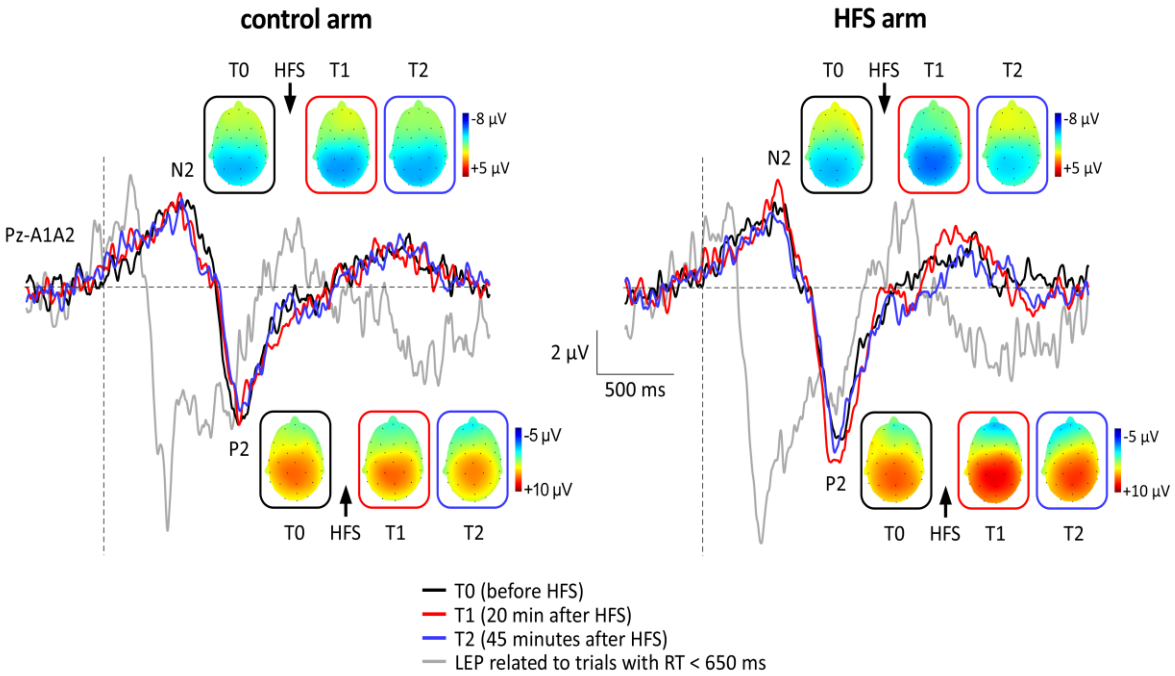

Figure 5. A and B. Effect of HFS on the intensity of perception (NRS) elicited by mechanical pinprick stimuli. Note the significant decrease on the control arm as compared to the HFS arm resulting in a greater heat sensitivity at the HFS treated arm. **C and D.** Effect of HFS on the intensity of perception (NRS) elicited by predominant thermal activation of C-fiber nociceptors. Note that, at both T1 and T2, heat perception

at the HFS arm is significantly larger as compared to the control arm. Asterisks refer to the results of the univariate within subjects tests; ** p < .01; *** p < .001.

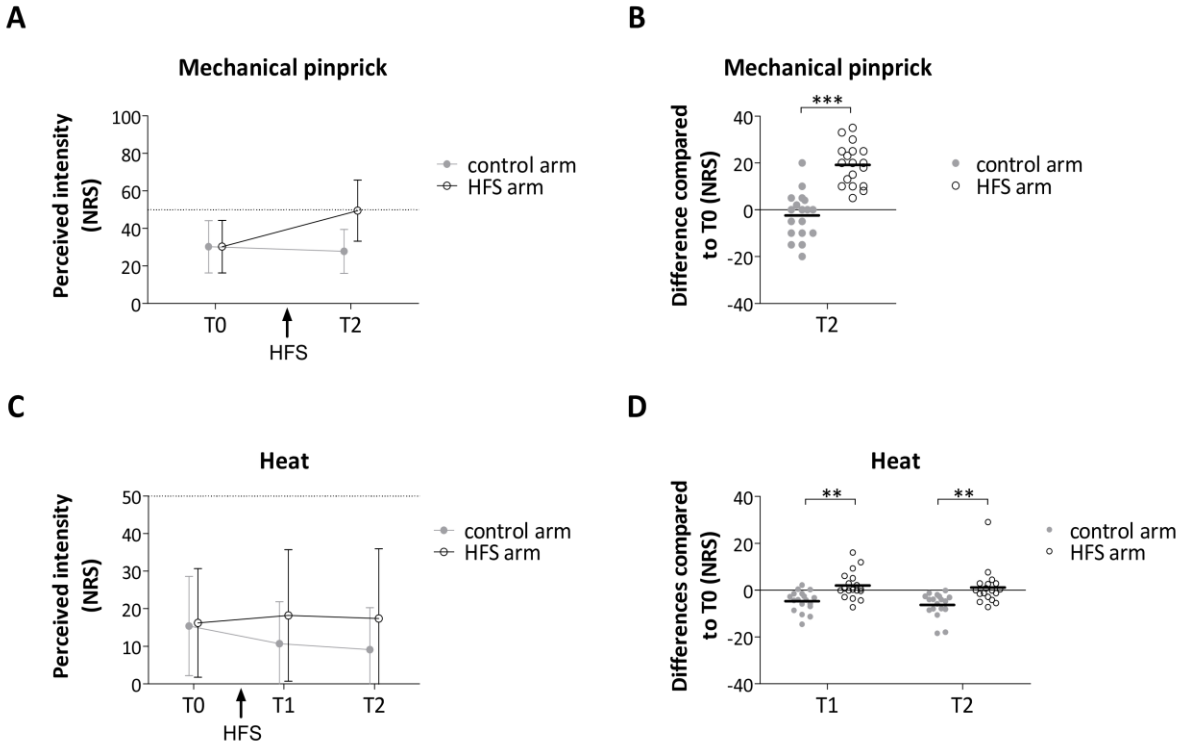

Figure 6. A. Frequency distribution of reaction times (RT) to transient high-intensity laser stimulation of the skin using a tiny skin surface area, across participants and conditions. The dashed line represents the latency cutoff (650 ms) above which RTs were considered to be compatible with the detection of unmyelinated C-fiber input. **B**

and C. Effect of HFS on the RTs of trials with RT ≥ 650 ms. Note the average decrease of RTs at T1 vs. T0 in response to heat stimuli delivered onto the HFS arm.

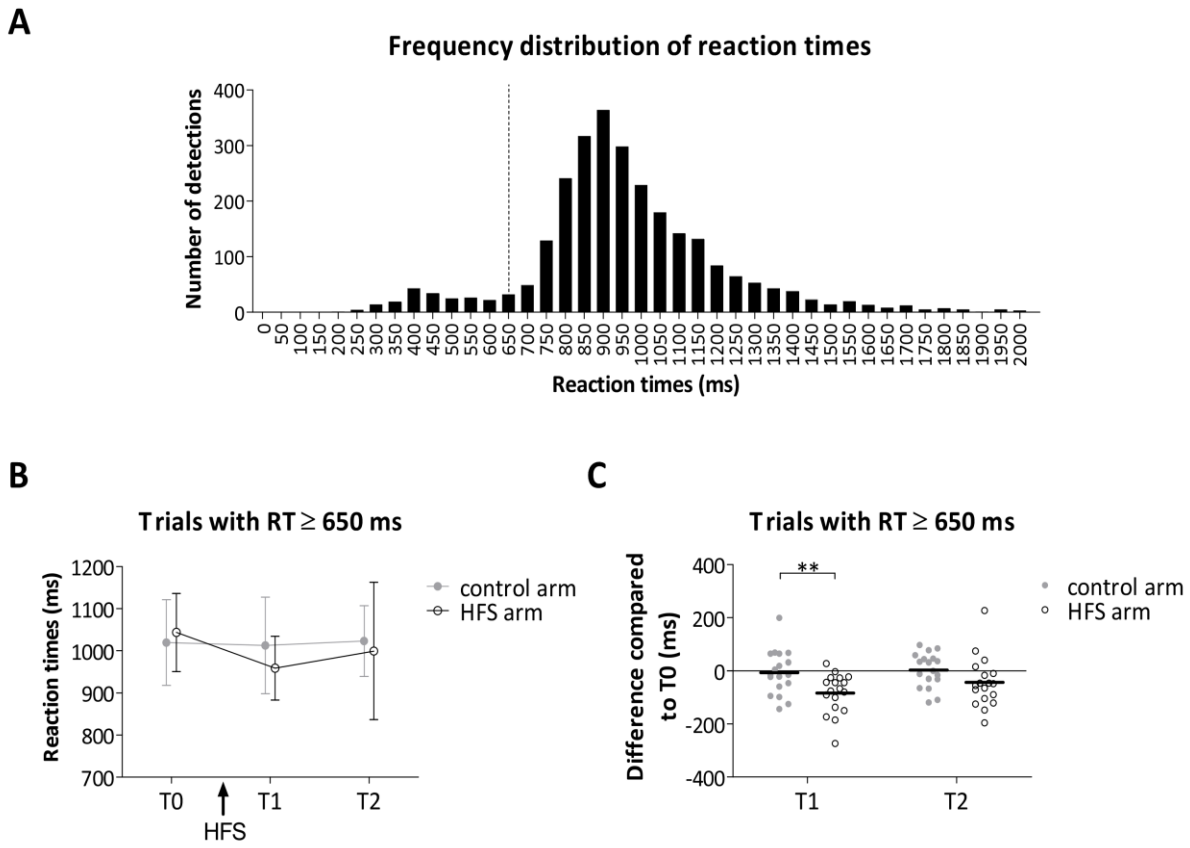

Figure 7. A. Stacked bar graphs showing for both arms in each condition the mean proportion of trials at which the stimuli were detected with a RT ≥ 650 ms, < 650 ms and undetected. **B.** Effect of HFS on the proportion of trials where RTs to laser stimuli were ≥ 650 ms, i.e. compatible with the conduction velocity of unmyelinated C-fiber nociceptors. **C.** Effect of HFS on the proportion of trials where RTs to laser stimuli were < 650 ms, i.e. compatible with the conduction velocity of thin myelinated Aδ-fiber

nociceptors. **D.** Effect of HFS on the proportion of trials in which the laser stimulus was not detected. Note that both at T1 and T2, a significantly larger proportion of trials were detected with C-fiber RTs at the HFS arm as compared to the control arm.

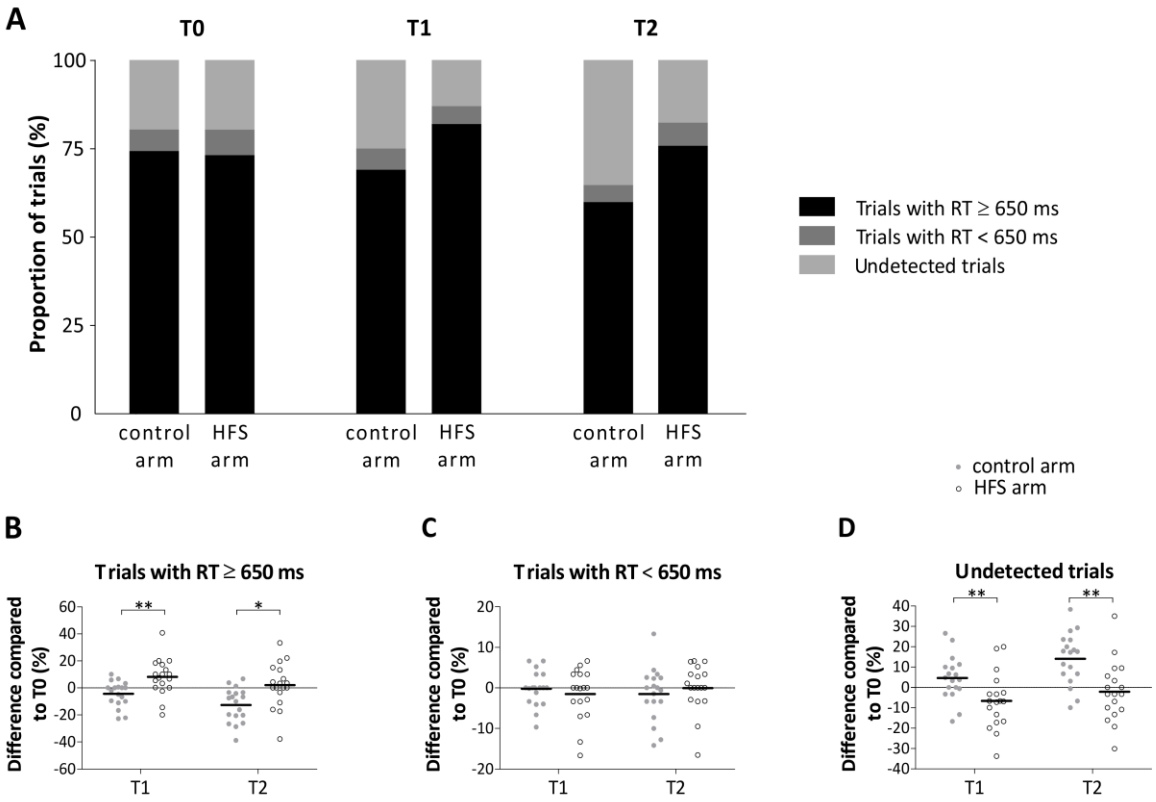

Figure 8. A and B. Effect of HFS on the magnitude of the N2 wave elicited by the predominant thermal activation of C-fiber nociceptors. The magnitude of the N2 wave was significantly enhanced both at T1 and T2 after HFS at the HFS treated arm as compared to control arm. **C and D.** The effect of HFS on the magnitude of the P2 peak

elicited by laser stimulation. The magnitude of the P2 peak tended to be greater at the HFS arm as compared to the control arm both at T1 and at T2, but this enhancement was not significant.